ENHANCED MULTIPHASE FLOW PREDICTIONS IN TWIN-SCREW PUMPS

by

Allan J. Prang

Manager of Engineering

Flowserve Canada Corporation

Brantford, Ontario, Canada

and

Paul Cooper

Consultant

Fluid Machinery Research, Inc.

Titusville, New Jersey

Al Prang is the Manager of Engineering for Flowserve Canada Corporation, in Brantford, Ontario, Canada. In his 36 years with the company, he has been involved with the R&D of various centrifugal and rotary pump designs for special applications. Recent R&D work has concentrated on difficult viscous and multiphase pumping applications with both centrifugal and rotary pumps. He has presented a number of papers on multiphase pumping and the handling of difficult liquids.

Mr. Prang received his Mechanical Engineering education at the Hamilton Institute of Technology and the University of Waterloo.

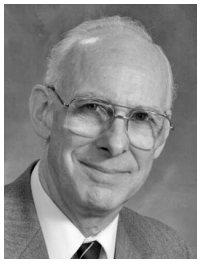

Paul Cooper is a Consultant with Fluid Machinery Research, Inc., in Titusville, New Jersey, and has spent 45 years in the pump industry. He retired in 1999 from 22 years of pump research and development at IDP, now part of the Flowserve Corporation. Prior to this, at TRW Inc., he performed the hydraulic design of aircraft fuel pumps and inducers as well as submersible centrifugal pumps for the oil field. More recently, he has included multiphase pumping as one of his areas of concentration, with emphasis on the design and performance prediction of twin-screw pumps.

Dr. Cooper is a Life Fellow of the ASME and is the recipient of ASMEs Fluid Machinery Design Award and their Henry R. Worthington Medal for achievement in the field of pumping machinery. He has written many papers in this field and is a co-editor of the Third Edition of McGraw-Hill's Pump Handbook.

ABSTRACT

In oil field applications it is often required to pump oil, gas, and water as mixtures rather than separating the fluid. Although the performance prediction of twin-screw pumps on liquids is well established, the prediction of performance of these pumps on multiphase mixtures presents a challenge. Test data of twin-screw rotary pumps are compared with predictions of performance over ranges of fluid viscosity and intake gas void fraction (GVF) from zero to 100 percent. The prediction method includes the effects of internal clearances, which can vary spatially, pressure distribution, laminar and turbulent internal leakage or "slip" flow, and viscous heating of the slip flow. The method predicts the experimentally observed variation of pump intake volume flow rate as pump pressure rise increases, namely:

- The traditional straight-line decrease for highly viscous, laminar, pure-liquid flow;
- The initially rapid decrease for low-viscosity, turbulent, pure-liquid flow; and
- The negligible decrease at high GVF and pressure ratio for all viscosities.

This ability to more accurately predict pump performance for the many combinations of operating conditions has enabled pump manufacturers to more accurately design the multiphase pump required for the intended duty.

INTRODUCTION

Twin-screw rotary pumps have historically been used to pump viscous liquids but are now often applied to handle multiphase fluids in oil and gas recovery applications. These pumps have the ability to pump fluids directly from the oil fields with a wide range of operating conditions. Liquids, oil, gas, and water mixtures or slugs of 100 percent gas can all be pumped at constant pressure with these screw pumps. The ability to maintain the full discharge pressure with all these fluids without the requirement for changes in operating speed is a significant advantage of these pumps.

Users and designers of pumping machinery are always concerned with the relevant performance characteristics. For twin-screw pumps, which are positive displacement machines, the variation of the delivered volume flow rate Q with the pressure difference Δp imposed across the pump is the major characteristic of interest (for definition of symbols, refer to NOMENCLATURE at end of paper). The resulting curve of Q versus Δp is found by subtracting from the displacement volume flow rate Q_d the leakage or slip $Q_{s,l}$ that is recirculated through the internal clearances back to the inlets of the screws. These inlets are at the outer ends of the screws shown in Figure 1, which is a side view of a typical, double-entry twin-screw pump. Historically, twin-screw pumps were used mainly for transferring viscous liquids and were designed accordingly (Karassik, et al., 2001). In this case, the slip $Q_{s,l}$ is laminar, which increases linearly with Δp, thus producing the straight line illustrated in Figure 2 for the performance characteristic curve.

However, this straight line does not apply for liquids of low viscosity, which have traditionally been transferred by rotordynamic (centrifugal) pumps. In this case the slip $Q_{s,l}$ is often turbulent and so tends to vary more as the square root of Δp, yielding a Q-Δp curve that is concave downward (i.e., it falls more

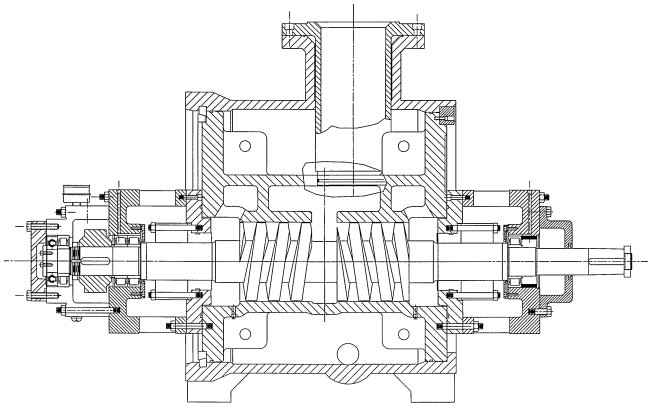

Figure 1. Multiphase Twin-Screw Pump Cross-Sectional View. (This side view shows one of the two meshing rotors, which contains two flights of screws, intake for each being at the outer ends and the discharge in the middle.)

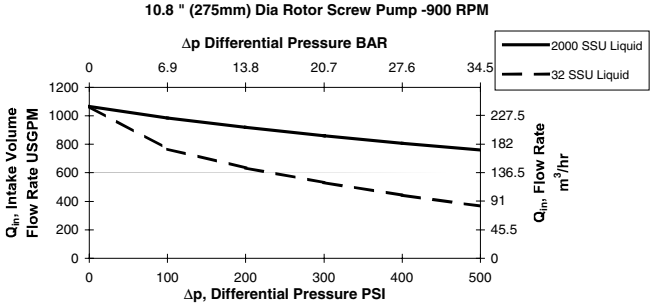

Figure 2. Performance Characteristics for High- and Low-Viscosity Liquids. (Test results for delivered flow rate against pressure rise. The upper plot is essentially the straight line of high-viscosity laminar slip flow, and the lower plot for low viscosity displays a short, straight portion of laminar slip followed by a curved turbulent portion.)

rapidly at first, as seen in Figure 2.) This is important, because users have found the advantages of the positive displacement configuration to be desirable in an increasing number of applications.

Further, in the past decade, many more applications have arisen that involve significant volumes of gas and liquid flowing together, so that this desirability has turned into necessity. Specifically, it was found that these pumps possess the ability to handle a wide and changing variety of single and multiphase flows—up to 100 percent gas—at any pressure rise from zero to the maximum design value. Early testing revealed a variety of multiphase performance curve shapes. An example of this early work is the test data of Figure 3, which were obtained for a small screw pump (Prang, 1991). For example, at high GVF, the total intake volume flow Q_{in} of both gas and liquid was found to change hardly at all with increasing Δp (GVF or gas void fraction is the ratio of ingested gas volume flow $Q_{g,0}$ to Q_{in}, expressed either fractionally or as a percentage.)

Pump power consumption obtained in the multiphase testing of the small screw pump is also shown in Figure 3. While power is not the focus of this paper but rather the correct prediction of the ingested (and therefore delivered) flow rate of the pump, Figure 3 does provide a look at the power behavior of these pumps, which can influence the choices that are made of pump size, speed, and the attendant volumetric efficiency. Because this is a positive displacement pump, the input shaft power P_s is simply $P_s = Q_d \Delta p + P_f$, where P_f is the fluid friction drag of the rotors, a small part of the total unless the liquid viscosity is unusually large. The term $Q_d \Delta p$ is not affected by GVF, as would be the case for a rotordynamic

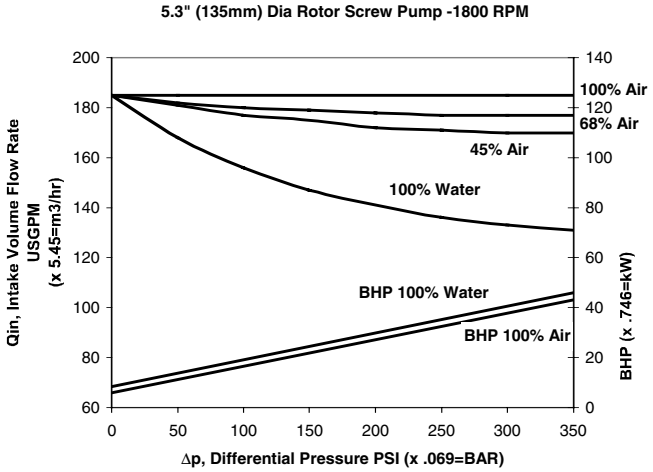

Figure 3. Multiphase Performance Characteristics (Water and Air). (Test results for a range of GVF shown as percentages. The curves for total ingested flow vary from that of low-viscosity liquids to no variation at 100 percent gas.)

machine (in which Δp depends on the average fluid density and the rotor tip speed.) Hence, the test results of Figure 3 show the straight-line result for power P_s versus pressure rise Δp; this line shifts by a very small amount with GVF, the difference being the change in the friction drag power P_f. Thus a screw pump can ingest slugs of gas, incurring neither the large spikes in shaft torque nor the need for a sudden increase in rotative speed in order to maintain Δp that would apply to rotordynamic pumps. Nevertheless, speed-varying devices are often supplied with screw pumps in order to accommodate the longer-term, more permanent changes in total intake volume flow, liquid viscosity, etc., that accompany changes in oilfield production rates.

This more recent multitude of applications and the corresponding variations of flow types and conditions have necessitated extensive upgrades to the traditional methods of predicting twin-screw pump performance characteristic curves. The physics of the laminar, turbulent, and multiphase flows within the pump had to be modeled, including both fluid mechanical and thermal considerations. Vetter and his students (Vetter and Wincek, 1993; Vetter, et al., 2000) recognized this, and they performed analytical studies of the slip phenomenon that took into account the effects of the liquid-leakage Reynolds number and the back-flowing leakage from the discharge side of the pump that performs the compression of the gas phase as the fluid advances from the intake to the discharge end of the screw profile. They verified these theories by extensive experimental research. Much of this insight is readily adaptable by pump manufacturers to the task of more accurately predicting the performance curves of twin-screw pumps.

MODELING THE SLIP

Volumetric Efficiency

The actual amount of fluid, both gas and liquid, which a positive displacement pump ingests is the most significant quantity in the performance prediction task. The volumetric efficiency:

$$\eta_v = \frac{Q_{in}}{Q_d} = \frac{Q_l + Q_{g,0}}{Q_d} = \frac{Q_l}{Q_d} \times \frac{1}{1 - GVF} = \frac{Q_d - Q_{s,1}}{Q_d} \qquad (1)$$

where $Q_{g,0}$ is the entering gas volume flow rate; and the intake gas void fraction:

$$GVF = \frac{Q_{g,0}}{Q_l + Q_{g,0}} \qquad (2)$$

expressed either fractionally or as a percentage; and $Q_{s,l}$ is the slip or internal leakage that emerges from the screws into their inlets, so that the ingested flow rate Q_{in} is less than the geometric displacement or swept volume flow rate Q_d.

Displacement or Swept Volume Flow Rate

Q_d relates to the size and speed of the pump as follows:

$$Q_d = 4\Omega D_1^2 \frac{P}{2}\varepsilon\left(1-\xi^2\right) = 4\Omega \frac{D_1^3}{2}\times\frac{P}{D_1}\varepsilon\left(1-\xi^2\right) = 4\Omega \frac{D_1^3}{2\left(n_l+1\right)}\times\frac{L_{sc}}{D_1}\varepsilon\left(1-\xi^2\right) \quad (3)$$

where Ω is equal to π times rpm/30, P is the pitch of the screw, ε is the fraction of annular space between the root and the tip of the screw threads that is not blocked by these threads, ξ is the ratio of the root diameter of the screw to the tip diameter D_t, L_{sc} is the length (= axial extent) of each pumping screw, and n_l is the number of "locks" or chambers created by the meshing screws. As indicated in Figure 1, each of the two screw rotors has two pumping screws, for a total of four flights of screw threads; this explains the appearance of the "4" in Equation 3.

Liquid Leakage

Computation of the slip flow rate $Q_{s,l}$ is fortunately greatly simplified when one realizes that the liquid phase will be centrifuged by the screws radially outward into the clearance gaps between the screw rotors and the surrounding casing bores. This is illustrated in Figure 4, which is a representation of the disc model proposed by Vetter, et al. (2000). Thus, the method of analysis predicts slip on the basis of only liquid leakage across the screw lands at the outer diameter of the screw rotor. Moreover, only that fluid $Q_{s,l}$ that leaks across the first land (nearest the intake end of the screw) reduces the ingestible volume flow rate below that of Q_d. In the earlier work (Vetter and Wincek, 1993), the convenient result was found that 80 percent of the slip flow passes over the screw lands through the tip clearance around the rotor, the rest passing through the clearances at the roots and flanks of the screws. However, this conclusion was reached for water flow. Since the length of the path of the slip flow through the tip clearance is greater than that through the root and flanks, as liquid viscosity increases, a reduced fraction of the total slip passes through the tip clearance. Thus, the tip leakage is computed assuming this result to be an empirical factor f_t times the total slip flow, where $f_t = 0.80$ for the high Reynolds number R-values associated with water and less than this for lower R. This simplifies the leakage analysis, as the root and flank leakages and geometry are more complicated than those associated with the tip clearance. Liquid sealing of the roots and flanks is thus also assumed, and this is admissible when one realizes that the liquid at the tips of the screw lands is carried to the roots and the flanks by means of the rotation.

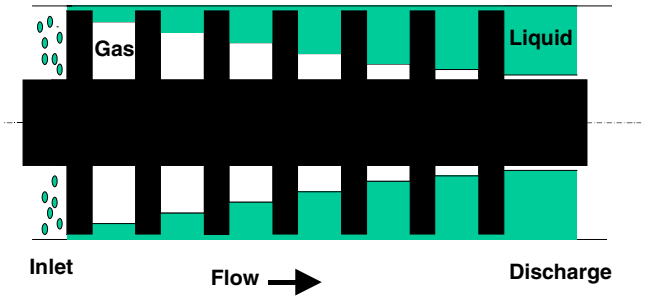

Figure 4. Model for Internal Leakage (Slip) and Compression of the Gas. (Liquid leakage seals the clearances and compresses the gas, this leakage and the corresponding pressure increase more rapidly toward discharge.)

Slip Through the Clearances

Thus the slip across the ith land (i.e., out of the ith lock) is represented by the following relationship:

$$Q_{s,i} = V_{lkg}\times A_{s,t}\times\frac{1}{f_t} = \sqrt{\frac{2\left(p_{i+1}-p_i\right)}{\rho_l\left(k_e + f\frac{l}{d_h}\right)}}\times A_{s,t}\times\frac{1}{f_t} \quad (4)$$

where the actual slip $Q_{s,l}$ affecting the pump volumetric efficiency is that occurring across the first land, i.e., the value of $Q_{s,i}$ for i = 1. ρ_l is the liquid density, k_e is the loss coefficient for entry of the flow into the clearance gap, $A_{s,t}$ is the effective leakage area in the tip clearance space and is approximately equal to $4\pi D_t\delta$, l is the length of the leak path across the screw land, i.e., the land width, the hydraulic diameter d_h of the leak path is twice the clearance δ in the gap between the land and the casing bore. The friction factor f is curve-fitted to the standard Moody diagram of f versus Reynolds number $R = V_{lkg}\, d_h/\nu$ (where ν is the kinematic viscosity) for laminar and turbulent flow through smooth pipes (Karassik, et al., 2001, page 8.35), the turbulent line first being extended monotonically through the transition region to the straight laminar line on that diagram. This representation of transition assumes that the rotation of the land will promote transition at lower values of R, which itself is based on the velocity of the leakage across the land V_{lkg}, which in turn depends only on the pressure drop across the land (Equation (4)). Moreover, this representation ensures stability in the computation of the performance curves, because both laminar and turbulent slip flow can exist over the range of a single curve of Q_{in} versus Δ_p.

Because the screw land is helical and not purely circumferential, the land effectively moves axially as the rotor revolves. This motion tends to oppose the leakage and should become more important as the pump rotational speed increases. However, analysis of this effect showed it to be small, so it was omitted from the computations. Comparisons of predictions with data are the final judge as to the validity of this approach, and these will be presented further on in this paper.

Pressure Development Through the Locks

The static pressure rises from the intake end of each screw flight to its discharge end, the flow being effectively pumped in parallel through all four screw flights. Referring to Figure 4, one sees that the entering gas is increasingly compressed in each chamber or lock formed by the meshing screws (represented by the series of discs shown), as it moves from the inlet to the discharge end, thereby reducing the exit value of the GVF accordingly. The compression in a given lock is affected by liquid that leaks back into this lock from the downstream one. As this compressing liquid must nearly fill the last lock, the rate of leakage flow passing from the discharge end of the screw and into the last lock is far greater than that passing into the first lock next to the inlet end of the screw. This means that the pressure rise across the land from the last lock into the discharge zone downstream of the screw flight is much greater than it is across the first land next to the inlet zone upstream. Solving Equation (4) for the pressure difference across land i shows that this difference increases rapidly with leakage (slip) flow $Q_{s,i}$:

$$\left(p_{i+1} - p_i\right) = \rho_l \times \left(k_e + f\frac{l}{d_h}\right)\times\frac{\left(\frac{Q_{s,i}}{A_{s,t}}\times f_t\right)^2}{2} \quad (5)$$

where the values of $Q_{s,i}$ are determined by the compression process of the gas flow rate $Q_{g,i}$ in terms of the pressures p_i, this gas flow rate being found from:

$$Q_{s,i} = Q_d - Q_l - Q_{g,i} \quad (6)$$

Q_l being the net liquid flow rate delivered by the pump. The pressure development through the locks reduces to two general shapes, namely those associated with the cases of all-liquid flow and multiphase flow:

• *All-liquid flow*—Here $Q_{g,i}$ in Equation (6) is zero, making the slip flow rate $Q_{s,i}$ the same for all the locks. Equation (5) thus gives the same pressure rise across each of the locks, yielding the stair-stepped, essentially straight-line pressure development versus axial position that is illustrated in Figure 5.

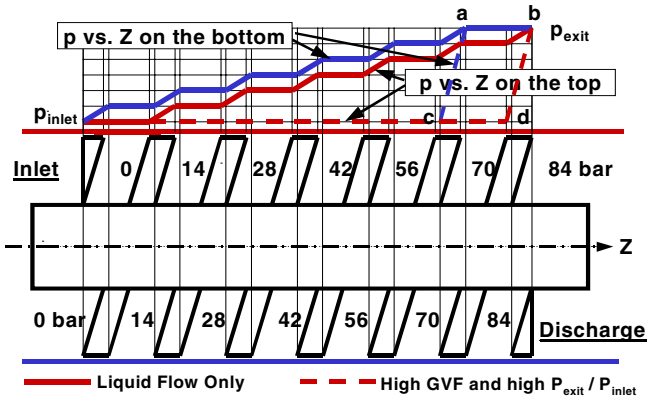

Figure 5. Pressure Development Through the Screw Rotors. (The pure-liquid and low-pressure-ratio multiphase case is seen as the "stair-stepped" curves that are straight lines on the average. The extreme case of 100 percent GVF and high pressure ratio shows no pressure increase until the last lock (next to the discharge) is reached.)

• *Multiphase flow*—Here the gas volume flow rate $Q_{g,i}$ will be reduced as depicted conceptually in Figure 4, thereby yielding increasing slip over the latter screw lands. This produces a parabolic-like curve of pressure versus axial position, a larger pressure rise occurring across the last land, and less across the first land (Prang, 1991; Vetter, et al., 2000). At the extreme of very high GVF and a very high ratio of pump outlet pressure to inlet pressure, all the pressure rise occurs across the last lock, as is also illustrated in Figure 5. Thus there is zero slip across the first lock, and the total ingested volume flow rate Q_{in} is equal to the pump displacement flow rate Q_d. This explains why, in Figure 3, the curve of Q_{in} versus Δp is so flat when GVF = 100 percent.

In the multiphase case, the gas compression process is assumed to be isothermal because the liquid and vapor phases have a sufficient interaction to enable the liquid to absorb the heat of compression of the gas with very little temperature increase. Therefore both phases are assumed to have nearly the same constant temperature. In this case, it is required that the gas volume from one lock to the next decrease as the ratio of the pressures:

$$Q_{g,i+1} = Q_{g,i} \times \frac{p_i}{p_{i+1}} \tag{7}$$

The overall pressure rise Δp is thus the sum of the pressure differences for all the locks:

$$\Delta p = \sum_{i=1}^{i=n_l} \left(p_{i+1} - p_i \right) \tag{8}$$

Effect of Rotational Speed

For high-GVF operation, computations utilizing the above slip and compression modeling display a strong effect of pump speed (rpm) on the resulting slip and therefore the curve of total inlet volume flow rate versus pump pressure rise Δp. This is illustrated in Figure 6 for the case of GVF = 95 percent. At 900 rpm the total inlet volume flow rate Q_{in} is obviously much less than that for the 1500 rpm case because the displacement volume flow rate Q_d varies directly with speed. However at the same maximum Δp of 500 psi, the increase in slip or fall-off of Q_{in} that occurs as Δp changes from zero to 500 psi is far more at 900 rpm than it is at 1500 rpm. This can be explained with reference to Equation (6), which at the same GVF and volumetric efficiency would require the same percentage increase in each term, namely, slip, displacement flow, ingested liquid flow, and gas flow rates. The correspondingly greater slip flow across the last lock (to fill the adjacent upstream lock as illustrated in Figure 4) would produce a greater pressure drop across the last land to drive this greater leakage flow. This also can be viewed as a larger pressure rise across the last land and out to the discharge zone. As the value of Δp across the whole pump is the same (500 psi) in both cases, there must be less pressure drop across the other lands and therefore less slip in the higher-speed case. Thus the volumetric efficiency actually increases with speed, as was found by Vetter and Wincek (1993) and Vetter, et al. (2000). However, no such increase would be predicted for the pure-liquid case at the same Δp, because the pressure change across each land is the same throughout the pump.

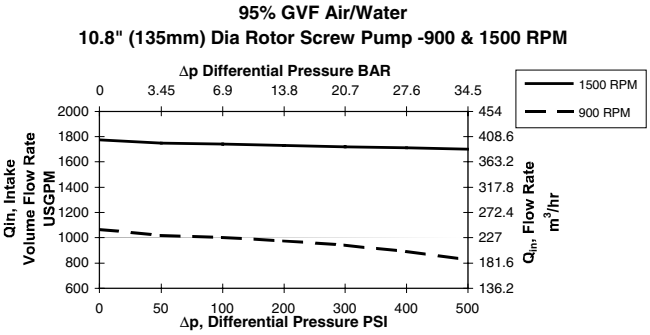

Figure 6. Effect of Speed on Multiphase Performance Predictions. (Increasing the speed not only increases the total ingested flow of gas and liquid, but it also reduces the fall-off of this flow versus pressure rise due to lower slip at higher speed.)

Spatial Variation of the Clearance

The pressure rise Δp of the pump imposes a radial load on the screw rotors that causes them to deflect in the bores (Prang, et al., 2002), making the tip gap clearance δ variable circumferentially as illustrated in Figure 7.

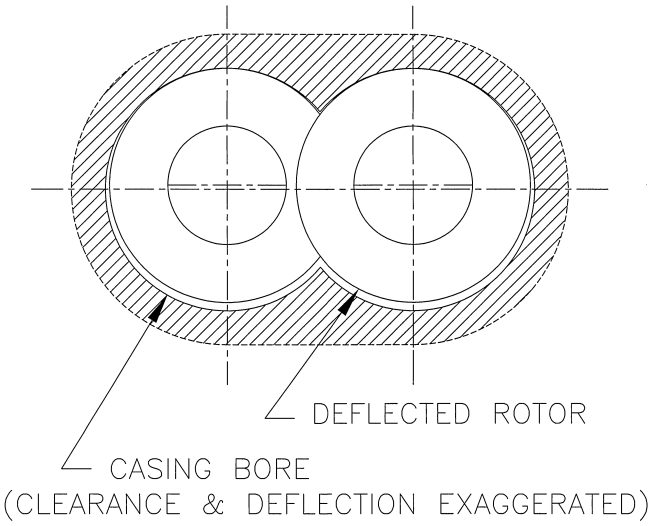

Figure 7. Nonuniform Clearance. (Loss of concentricity of the screw rotors in the casing bores due to offsetting and/or deflection of these rotors under the load due to the pump pressure rise can result in an increase of slip flow.)

The existence of this load can be deduced from Figure 5, e.g., the two curves of pressure development versus axial position for zero GVF are displaced from each other due to the helical disposition of the screw and the fact that the pressure is constant

within any one lock. The upper (stair-stepped) curve is obtained along the bottom of the screw, while the similar but displaced lower curve is obtained along the top. The result is therefore a radial force F_r, which is quantified as follows:

$$F_r = PD_t \times (1+\xi) \times \Delta p \tag{9}$$

where P is the screw pitch. Figure 5 also depicts a similar shift in the pressure distribution for the extreme case of 100 percent GVF and very high pressure ratio across the pump. The resulting radial load on each double-entry screw rotor is the same in both cases and is given by Equation (9).

This deflection of the rotors causes more slip than if δ were constant at its circumferentially averaged value. This increase in slip is quite significant in the case of laminar slip flow, as is evident from the form that Equation (4) (with the approximation of $4\pi D_t\delta$ for the tip leakage area $A_{s,t}$) takes when the flow is laminar, namely:

$$Q_{s,i} = \frac{(p_{i+1} - p_i)4\pi D_t \delta^3}{12\mu l} \tag{10}$$

where μ is the absolute viscosity of the liquid. In this case, referring to Figure 7, if the rotor were fully deflected to the point of zero clearance (δ = 0) on one side and δ = twice the undeflected clearance δ_u on the opposite side, the cubic variation of δ would locally yield eight times leakage rate where $\delta = 2\delta_u$ and zero leakage where $\delta = 0$. This could easily double the slip that would occur if the clearance δ were uniform circumferentially and equal to δ_u. Thus the performance computations assume typical deflection of the rotor and make empirical adjustments that are a function of Reynolds number R, effectively increasing the clearance δ associated with Equation (4) above the average value δ_u.

Viscous Heating

Another phenomenon associated with laminar slip flow and the correspondingly high liquid viscosities and low leakage Reynolds numbers is the viscous heating that effectively reduces the viscosity of the liquid, thereby allowing greater slip. This heating is caused by the shearing of the leaking liquid as it passes through the clearance at the tip of the screw. The resulting average viscosity in the clearance gap is found iteratively from the viscosity-versus-temperature relationship of the liquid. The temperature rise of the liquid in the gap is found from the drag power that arises from the tangential shear stress in the gap divided by the mass flow rate of the leakage and its specific heat. The average viscosity computed in this manner is the value of viscosity that is used for computing the friction factor f (R) in Equation (4) and the resulting slip.

Effect of Pressure Ratio

In many field applications, the absolute inlet pressure p_{in} to the multiphase pump is significant, often several atmospheres. This is often not reproduced in shop testing of the pump prior to shipment, where p_{in} is commonly near atmospheric pressure. The rated pump pressure rise $\Delta p = (p_{out} - p_{in})$ is always reproduced in the shop tests but the pressure ratio, pressure ratio (PR) = p_{out}/p_{in}, is larger for the shop tests than it is in these field applications. However, the pump is selected to meet the specified conditions of service from the field. The present performance prediction method is applied to confirm that the chosen pump configuration will indeed meet the specified conditions of service, which include the field pressure ratio. Figure 8 shows predictions made by the present method (which includes this PR-effect in the performance modeling as evidenced by Equation (7)). Shown in the figure are curves of pump flow rate versus Δp for three values of PR that cover a typical range of this quantity. As PR increases from 3.3 to the typical shop-test value of 34.3, the pump delivers more flow. Figures 4 and 5 are an aid in understanding why this happens. For example, if p_{in} were extremely high—say, much greater than Δp—there would be negligible compression, and the decrease of the gas volume from inlet to outlet depicted in Figure 4 would not occur, i.e., the gas would not be compressed very much at all. The resulting pressure development versus axial position would then be very nearly the same as depicted in Figure 5 for the zero-GVF case. This puts more pressure difference across the first lock—with the correspondingly reduced output due to the greater slip back to the inlet. But the higher pressure rise across the last lock that is typical of high GVF and significant pressure ratios is very much reduced in the field if the inlet pressure is greater than it is in the shop tests. This has the added benefit of producing lower pressure pulsations and potentially less mechanical vibration in the field.

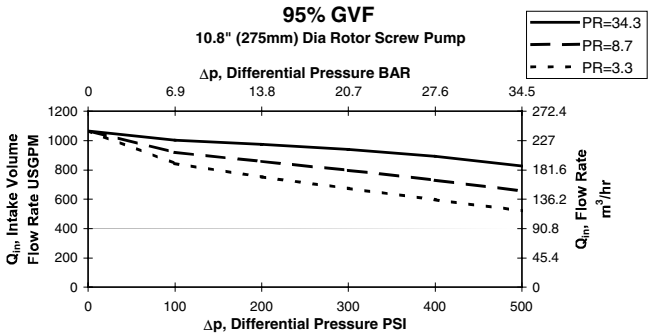

Figure 8. Effect of Pressure Ratio. (An increase in the pressure ratio reduces the slip flow, thereby increasing the output at a given pump pressure rise.)

Porting

When the forementioned vibration becomes an issue for successful deployment of multiphase screw pumps, it is common practice to locally increase the clearance at the outer diameter of the screw flights near their discharge ends. This "porting" reduces the pressure rise across the last lock, which as has been explained can be quite large at high GVF and high pump pressure ratio. While not specifically treated in the computations according to the foregoing theory, the effect of porting can be approximated by slightly decreasing the number of locks employed in these computations.

Remarks on the Slip Model

The foregoing phenomena have been coded into a working performance-prediction program for both liquid and multiphase screw pumps. While the emphasis in this paper has been on the slip model, as a means of predicting pump flow rate, the code also includes the prediction of power consumption, which together with the flow rate results also implies overall pump efficiency. The program has been run for many cases, some of which are presented in the following section in order to assess the validity of the theory. As more comparisons with test data become available, it may be necessary to alter such things as the assumptions about transition from laminar to turbulent flow, wherein the rotational Reynolds number may play a more significant role than has here been assumed relative to the leakage throughflow Reynolds number R. It is a fairly simple matter to upgrade the code with such improvements. This is a necessary and typical approach to learning about how any fluid machine performs and so can serve as an aid in the design process.

EXPERIMENTAL VALIDATION OF MODEL

A number of rotary screw pumps have been tested at various operating conditions to confirm performance and validate the flow prediction model. Unfortunately, factory testing of these pumps is often limited by flow and power limitations as well as environmental restrictions on the type of fluids that can be handled. Therefore, the validation tests conducted on multiphase have been limited to air/water multiphase mixtures. Limitations in accurately

measuring multiphase flow and controlling stable operating conditions in the field make field validation of other conditions impractical, thus limiting validation of the model to the factory testing at this time.

The discussion in the previous section confirms that three distinct and different flow regimes through the clearances result in different performance characteristics for the different operating conditions. These conditions are:

- *Viscous liquid operation*—Linear performance characteristic
- *Low viscosity liquid operation*—Concave downward characteristic
- *Multiphase operation*—Linear or concave upward characteristic

The following factory test results show close agreement with the flow prediction model, thus validating this model and confirming the different flow characteristics.

Viscous Liquid Operation

As indicated, screw pump performance with viscous liquids is characterized with laminar flow of the slip leakage back through the internal clearances, resulting in a linear relationship between slip and differential pressure and a linear performance curve. Figure 9 shows a relatively linear relationship between the differential pressure and the intake volume flow rate. This curve shows the actual performance versus the predicted performance of a small screw pump with 6 inch (150 mm) diameter rotors, when operating on oil with a viscosity of 857 SSU (185 cp), at 880 rpm. The performance predicted by the model for two different screw clearances shows the sensitivity of the pump to clearance variation. The actual measured performance is shown with the diamonds and the solid and dashed lines show the predicted performance at 0.013 inch (0.33 mm) screw clearance and 0.015 inch (0.38 mm) clearances, respectively. Note that all clearances indicated are diametral clearances between the rotor and the bore.

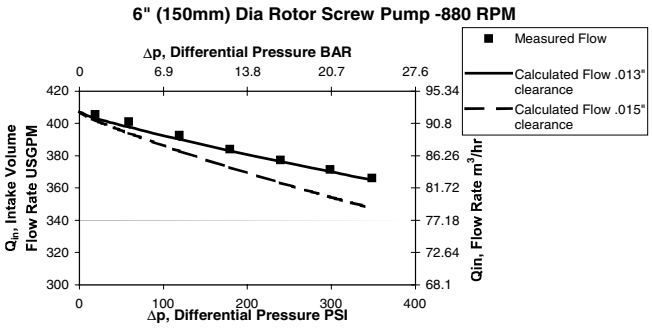

Figure 9. High-Viscosity Liquid Performance. (The essentially straight-line characteristics of laminar slip flow are well predicted. Note the sensitivity of the predictions to the clearance between the screw lands and the casing.)

The model does predict a slight change in the slope of the curve at lower differential pressure. This is due to the viscous heating effect discussed in the previous section. At higher differential pressures there is sufficient slip through the clearances to overcome this effect and produce the linear slip characteristic shown.

This curve confirms good agreement between the test data and the performance predicted for the 0.013 inch screw clearance, which was the approximate clearance of the pump tested.

Low Viscosity Liquid Operation

With low viscosity liquids, screw pumps exhibit a nonlinear slip characteristic due to the turbulent flow characteristics in the screw clearances. This nonlinear flow characteristic is shown in Figure 10. This curve shows the actual performance versus the predicted performance of a multiphase screw pump with 10.8 inch (275 mm) diameter rotors, when operating on water, at 900 rpm. The performance predicted by the model for two different screw clearances is shown and again confirms the sensitivity of the pump to clearance variation. The actual measured performance is shown with the diamonds, and the solid and dashed lines show the predicted performance at 0.027 inch (0.69 mm) screw clearance and 0.030 inch (0.76 mm) clearance, respectively. The slope of the curve is steep at low differential pressures but gradually reduces as the differential pressure is increased, confirming the transition from laminar to turbulent slip flow through the clearances.

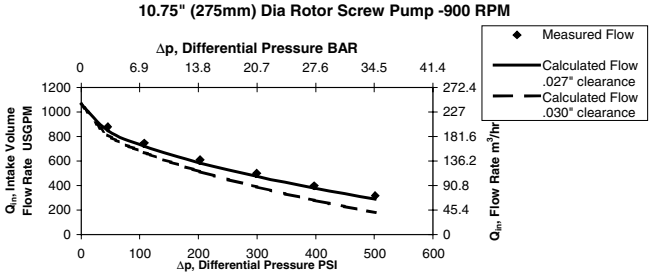

Figure 10. Low-Viscosity Liquid Performance. (The concave downward shape of the turbulent slip-flow case is evident, as is the rather straight initial portion indicating laminar slip at the low values of pressure rise.)

The actual performance agrees closely with the predicted performance at 0.027 inch (0.69 mm) screw clearance, thus confirming the model prediction with low viscosity liquids. The predicted change in slope of the curve with increasing differential pressure is also validated.

Multiphase Performance—Air/Water Mixture

As indicated in the previous explanations, the screw pump performance on multiphase fluids is more complicated, and the shape of the curve can vary from concave upward to almost linear with little slip. The performance characteristics depend on many factors including rotating speed, differential pressure, GVF, liquid viscosity, and screw clearances. Comparisons of several different pumps and operating conditions are shown to illustrate the effects of some of these variables.

58 Percent GVF

Figure 11 shows the actual performance of a multiphase screw pump with 10.8 inch (275 mm) diameter rotors, when operating on 58 percent air/water mixture, at 900 rpm. This performance is compared to the flow rates predicted by the computer model, shown again for two different screw clearances. The actual measured performance is shown with the diamonds, and the solid and dashed lines show the predicted performance at 0.025 inch (0.64 mm) screw clearance and 0.028 inch (0.71 mm) clearance, respectively.

As explained, lower GVF values result in less gas volume to compress, and the slip through the clearances is therefore less than with pure liquid but greater than with the higher GVF fluids. The actual test data show good correlation with the predicted performance at the higher differential pressure but does show slight deviation from the model at the lower differential pressures. The slight capacity rise at very low pressures, predicted by the model, is not apparent in the test data but few test points are available in this region to verify this characteristic.

86 Percent GVF

Figure 12 shows the actual performance of a multiphase screw pump with 10.8 inch (275 mm) diameter rotors, when operating on 86 percent air/water mixture, at 903 rpm. The computer predicted

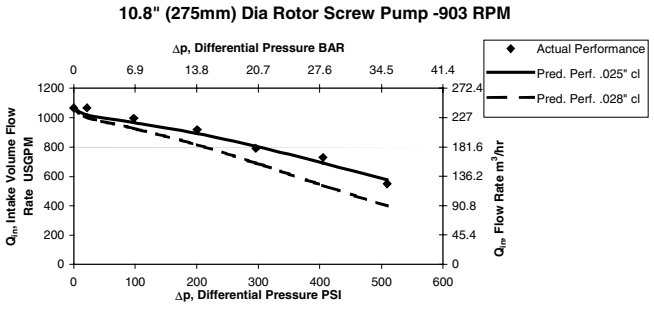

Figure 11. Multiphase Performance—Air and Water at 58 Percent GVF. (Comparison of test data with predictions. Note the importance of clearance on the predictions. Actual clearance may be slightly larger than that of the predictions.)

performance is also shown for two different screw clearance values. The actual measured performance is shown with the diamonds, and the solid and dashed lines show the predicted performance at 0.028 inch (0.71 mm) screw clearance and 0.030 inch (0.76 mm) clearance, respectively.

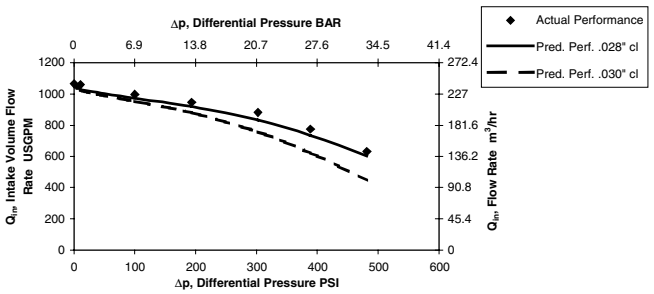

Figure 12. Multiphase Performance—Air and Water at 86 Percent GVF. (Comparison of test data with predictions. Note the importance of clearance on the predictions. Actual clearance may be slightly larger than that of the predictions.)

This performance shows less reduction in flow rate as the pressure increases than the comparable performance at the lower 58 percent GVF. A slight rise in capacity at low pressure is again predicted by the model but is at even lower pressure. The lack of sufficient test data in this region again prevents verification of this characteristic, but this should not be a concern, as the equipment is not normally operated at these low differential pressures.

This curve shows good correlation of the test data to the predicted performance at the 0.028 inch (0.71 mm) screw clearance, again confirming the capabilities of the model to predict performance on multiphase fluids.

93 Percent GVF

Figure 13 shows the performance of a larger multiphase screw pump with 15.0 inch (380 mm) diameter rotors, when operating on 93 percent air/water mixture, at 900 rpm. The actual measured performance is shown with the diamonds, and the solid and dashed lines show the predicted performance at 0.028 inch (0.71 mm) screw clearance and 0.030 inch (0.76 mm) clearance, respectively.

This performance indicates an even flatter characteristic than the lower GVF curves confirming less slip than the lower GVF conditions. The slight rise in capacity at low pressures is again predicted by the model but again is not apparent in the test data.

Again this curve shows good correlation of the test data to the predicted performance at the 0.028 inch (0.71 mm) screw clearance, confirming the capabilities of the model to predict performance on multiphase fluids at higher GVF values.

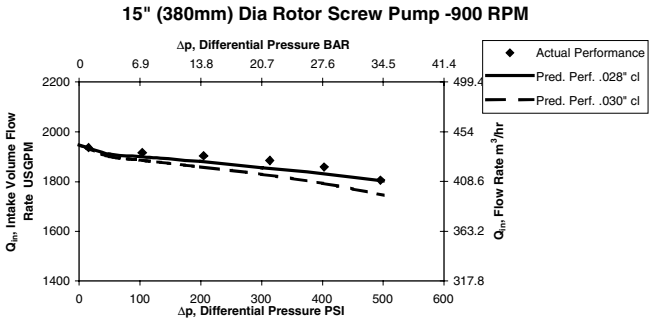

Figure 13. Multiphase Performance—Air and Water at 93 Percent GVF. (Comparison of test data with predictions. Actual clearance may be slightly larger than that of the predictions. Note that less fall-off in performance [less slip] is found both experimentally and via predictions as GVF increases [Figures 11 through 13.])

CONCLUSIONS

A theory and computational program for the performance of rotary positive displacement pure liquid and multiphase double-entry twin-screw pumps has been developed. The effects of gas void fraction, liquid viscosity, specific heat, pressure ratio and pressure rise, pump rotational speed, size, screw geometry, and constant and variable internal clearances have been modeled and coded into the program. Basic to the method is the assumption that the slip flow or internal leakage through the clearances is purely liquid. Also, this leaking liquid performs the function of compressing the gas as it proceeds axially through the meshing screws. The primary outputs of the method are the resulting constant-speed characteristics of total ingested volume flow rate of both gas and liquid versus the imposed differential pressure or pressure rise. The attendant power consumption is also predicted and is largely the product of the displacement or swept volume flow rate times the pressure rise. The known behavior of many aspects of the pumping done by these machines has been simulated, including the following effects:

- The change from an essentially linear development of pressure versus axial position for pure-liquid flow to a parabolic development at GVF > 0, the slip flow back to the inlet (that reduces volumetric efficiency) being reduced by consequent lower pressure drop across the screw lands adjacent to the pump intake zone.

- The effect of pump overall pressure ratio for GVF > 0, wherein the parabolic distribution of pressure is accentuated at high PR and tends toward the linear, pure-liquid distribution at low PR.

- The improvement in volumetric efficiency with increasing rotational speed at constant GVF and pump pressure rise.

- Simulation of nonuniform clearances around the rotor, typically caused by the deflection of the rotors due to the pressure rise across the pump.

- Reduction of the effective viscosity of the slip flow arising from heating due to the viscous drag of fluid on the screw lands.

It was found possible to test most of these effects through experiments on actual production pump models, the following comparisons of predicted performance characteristics with the test data having been made with good success:

- *High-viscosity, pure-liquid flow*—The essentially straight-line, traditional fall-off of flow rate with increasing pressure rise Δp was well simulated.

- *Low-viscosity, pure-liquid flow*—The concave-downward fall-off of flow rate with Δp due to turbulent slip was correctly modeled. The initial portion of this curve was steeper and tended to be straight, indicating the presence of laminar slip in this region.

• *Multiphase flow at three values of GVF*—Both the predictions and the tests showed good agreement, which included the change of the characteristic curve from being similar to the low-viscosity pure-liquid case at 58 percent GVF to an almost flat curve (very little slip at all Δp) at 93 percent GVF.

A change in operating conditions in the field that produces a lower liquid viscosity is a serious development that can significantly reduce the capacity of a twin-screw pump that has performed as intended until the change. In an interesting twist, lowering the liquid viscosity seriously impairs the performance of a twin-screw pump whereas the same change enhances that of a rotordynamic (centrifugal) pump. If these two designs could be used interchangeably, the problem of low liquid viscosity could be overcome by changing the pump type. This is precluded by the quite different hydraulic coverage of the two designs, thus illustrating both the necessity for and the utility of the enhanced performance prediction capability for twin-screw pumps that has been reported here.

NOMENCLATURE

$A_{s,t}$ = Effective leakage area in the tip clearance space
D_t = Tip diameter of the screw
d_h = Hydraulic diameter
f = Friction factor
f_t = Ratio of tip screw tip leakage to total leakage through all clearances
F_r = Radial force
GVF = Intake gas void fraction expressed as percent or a fraction
k_e = Loss coefficient for entry of the flow into the clearance gap
l = Length of the leak path across the screw land
L_{sc} = Length (= axial extent) of each pumping screw
n_l = Number of "locks" or chambers created by the meshing screws
P = Pitch of the screw
P_f = Fluid friction drag of the rotors
P_s = Input shaft power
p_{in} = Absolute inlet pressure
p_{out} = Absolute outlet pressure
PR = Pressure ratio = p_{out}/p_{in}
Δ_p = Pressure difference across the pump
Q = Delivered volume flow rate
Q_d = Displacement volume flow rate
$Q_{s,1}$ = Leakage or slip across the first screw land
$Q_{s,i}$ = Leakage or slip across screw land i
Q_{in} = Total intake volume flow
$Q_{g,0}$ = Ingested gas volume flow
R = Reynolds number
V_{lkg} = Velocity of the leakage across the land
δ = Clearance in the gap between the land and the casing bore
δ_u = Undeflected clearance
ε = Fraction of annular space between the root and the tip of the screw threads that is not blocked
ξ = Ratio of the root diameter of the screw to the tip diameter
η_v = Volumetric efficiency
μ = Absolute viscosity of the liquid
ν = Kinematic viscosity
ρ_l = Liquid density
Ω = Angular speed of the pump (= $\pi \times$ rpm/30)

REFERENCES

Karassik, I., Messina, J., Cooper, P., and Heald, C., 2001, *Pump Handbook*, Third Edition, New York, New York: McGraw Hill.

Prang, A., November 1991, "Rotary Screw Pumps for Multiphase Products," *World Pumps*, pp. 18-23.

Vetter, G. and Wincek, M., 1993, "Performance Prediction of Twin Screw Pumps for Two-Phase Gas/Liquid Flow," *Pumping Machinery—1993*, FED-*154*, ASME, pp. 331-340.

Vetter, G., Wirth, W., Körner, H., and Pregler, S., 2000, "Multiphase Pumping with Twin-Screw Pumps—Understand and Model Hydrodynamics and Hydroabrasive Wear," *Proceedings of the Seventeenth International Pump Users Symposium*, Turbomachinery Laboratory, Texas A&M University, College Station, Texas, pp. 153-169.

Prang, A. J., Hartt, R., and Cooper, P., 2002, "Optimizing Multiphase Pumping Equipment for Actual Field Conditions," *BHR Group 2002 Multiphase Technology*, pp. 195-215.